ARTICLES
PUBLISHED ONLINE: 27 FEBRUARY 2017 | DOI: 10.1038/NCLIMATE3225
nature climate change

Slower snowmelt in a warmer world

Keith N. Musselman*, Martyn P. Clark, Changhai Liu, Kyoko Ikeda and Roy Rasmussen

There is general consensus that projected warming will cause earlier snowmelt, but how snowmelt rates will respond to climate change is poorly known. We present snowpack observations from western North America illustrating that shallower snowpack melts earlier, and at lower rates, than deeper, later-lying snow-cover. The observations provide the context for a hypothesis of slower snowmelt in a warmer world. We test this hypothesis using climate model simulations for both a control time period and re-run with a future climate scenario, and find that the fraction of meltwater volume produced at high snowmelt rates is greatly reduced in a warmer climate. The reduction is caused by a contraction of the snowmelt season to a time of lower available energy, reducing by as much as 64% the snow-covered area exposed to energy sufficient to drive high snowmelt rates. These results have unresolved implications on soil moisture deficits, vegetation stress, and streamflow declines.

In many regions of the world, the melt of accumulated winter snowfall provides the dominant source of annual water for streamflow and groundwater recharge. This seasonal water resource is one of the fastest changing hydrologic features under global warming[1] with broad impacts on economies[2], ecosystem function[3] and flood hazard[4]. Warmer temperatures reduce historical snowpack volume and persistence[5] by shifting precipitation from snowfall to rain and causing snowmelt to occur earlier[6]. By the end of the twenty-first century, the peak flow of many North American and European rivers is expected to occur 30–40 days earlier as a result of earlier snowmelt[7,8]. This example is one of many well-known relationships between snowmelt timing and seasonal trends in soil moisture[9,10], evapotranspiration[11,12], streamflow[13,14], and wildfire activity[15,16]. Projected changes in snowmelt timing will have pervasive hydrological and ecological impacts; however, the nature of the effects will depend on the magnitude of future snowmelt rates. The rate of snowmelt directly impacts streamflow[17] with attendant connections to water yield and flood risk, all of which are important considerations for water resource management. While there is general consensus that projected warming will cause earlier snowmelt, how snowmelt rates will respond to climate change is poorly known and critical to future water assessments[18].

Climate warming can impact snowmelt rates in contradictory ways. Warming can enhance snowmelt by increasing the energy available to a saturated snowpack such as in the case of higher melt-season air temperature or a rain-on-snow event[19]. By contrast, the resulting snowpack depletion contracts the length of the snow season, causing melt to occur earlier, and potentially at lower rates under conditions of lower available energy (for example, net solar radiation)[20]. This association between earlier snow disappearance and lower snowmelt rates has been inferred by previous studies including an analysis of historical US snowpack observations[21]. Additionally, changes in precipitation caused by climate change[22] can further enhance or reduce spring snowmelt rates, depending on whether precipitation changes are manifested as increases or decreases in snowfall[20,23]. Thus, if lower spring snowmelt rates due to reduced snow-cover persistence are not compensated by snowfall increases and/or warming-induced melt increases, snowmelt may be slower in a warmer world. A thorough evaluation of how regional snowmelt rates will change in a warmer world requires resolving these often-compensatory climate and snowpack dynamics across fine spatial scales and climatic gradients that determine snowmelt regimes in both a current and future climate.

In this study, we use a mix of historical data analysis and controlled regional climate model simulations to test a hypothesis of slower snowmelt in a warmer world. We pursue three related analysis strategies: a station-based evaluation of daily snow depletion; an analysis of high-resolution regional climate simulations of snowmelt; and a comparison of historical snowmelt simulations with those from the model run with imposed climate perturbations.

First, to understand relationships between snowmelt rates and snowpack volume as it relates to the timing of snow-cover depletion, we evaluate historical observations of the daily change in snow water equivalent (SWE) (that is, the ablation rate; see Methods) from 979 automated snowpack monitoring stations in western North America. Second, to determine whether the observed, point-scale results are evident at regional to continental scales, we repeat the station-based analysis using high-resolution regional climate simulations from the Weather Research and Forecasting (WRF) model over western North America[24]. The physical basis, fine grid spacing, and large geographic extent of the WRF simulations enable representation of the processes, climate, terrain and land cover that shape regional snow water resources[25]. Third, to quantify changes in simulated snowmelt rates in response to climate warming, we impose climate perturbations on the historical WRF simulations[24] to simulate future (2071–2100) climate sensitivity to the Representative Concentration Pathway 8.5 greenhouse gas concentration trajectory[26]. The three analysis strategies provide complementary lines of evidence that illustrate a general tendency for slower snowmelt in a warmer world.

Observations and model assessment

Figure 1 presents an analysis of daily snowpack depletion from both historical SWE observations and WRF simulations across western North America, demonstrating lower ablation rates in locations with less SWE. The four cumulative distribution function (CDF) curves from historical station data (Fig. 1a) show a clear positive relationship between ablation rates and snowpack magnitude. Specifically, deeper, prolonged snowpack exhibits higher ablation rates than sites with historically shallower snowpack (Fig. 1;

National Center for Atmospheric Research, Boulder, Colorado 80307-3000, USA. *e-mail: kmussel@ucar.edu

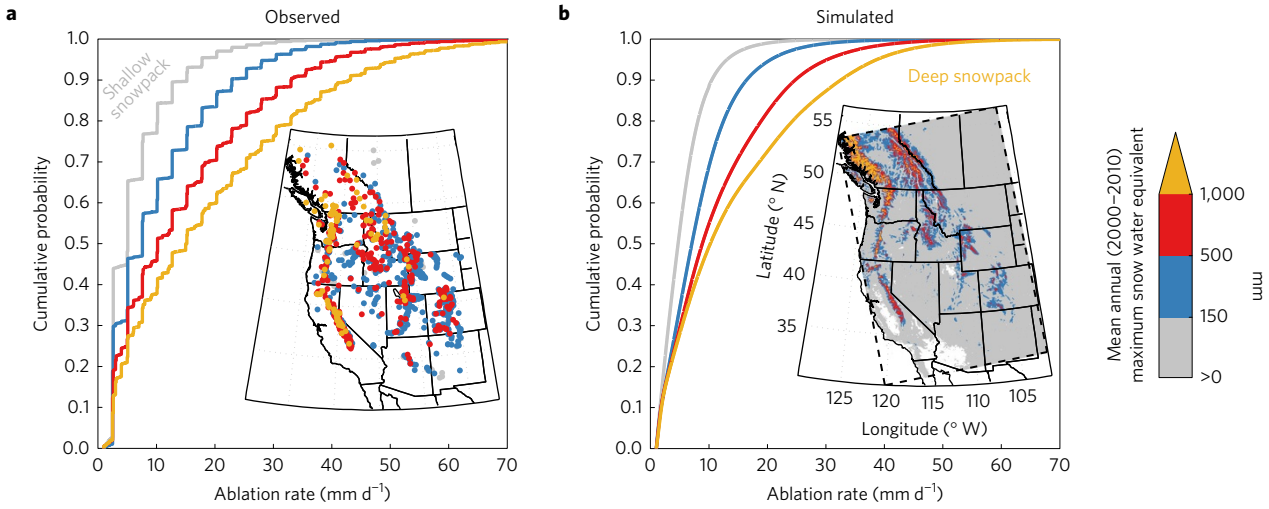

Figure 1 | Observations and model simulations of snow water equivalent (SWE) across western North America, for the period October 2000 until September 2010, demonstrate lower ablation rates in places with less SWE. a, Cumulative probability distributions of observed SWE ablation rates (mm per day) at the telemetry station locations for four snow classes binned by mean annual maximum SWE. **b**, The cumulative probability distribution of SWE ablation rates simulated by the WRF model using the same four snow classes. The inset maps in **a** and **b** denote the stations and grid cells associated with each of the four snow classes. Ablation rates shown are restricted to values ≥1 mm per day to simplify comparisons between the model, which effectively does not have a lower ablation limit, and the measurements, which are limited by sensor accuracy.

compare the curves for deep snowpack (orange) with those for shallow snowpack (grey)). These positive relationships between snowmelt rates and SWE volume are consistent with previous analyses of US snowpack observations[21]. To be clear, deep snow does not melt faster than shallow snow given equal energy input—in fact, deeper snowpack can require greater energy input to overcome cold content and liquid water holding capacity and initiate snowmelt runoff[27]. The observed positive relationship between ablation rates and SWE occurs because deeper snowpack persists until late spring and summer when energy availability is high. The empirical relationship suggests that melt could be slower in a warmer climate characterized by reduced SWE, earlier snowmelt, and less spring snow-cover. Future melt rates will be determined by changes in climate and the snowpack energy balance and therefore are best addressed with physically based climate and land-surface models.

The four ablation rate CDF curves from the WRF simulations (Fig. 1b) support results from the observational analysis (Fig. 1a)—that in regions with deeper, more persistent snow-cover, ablation rates are higher than in regions with shallower snowpack. The similarities between the observed (Fig. 1a) and modelled (Fig. 1b) ablation rate CDF curves provide confidence in the capacity of WRF to simulate the snowmelt dynamics explained in this paper (see also ref. 24).

Response of snowmelt rates to warming

Figure 2 illustrates changes in snowmelt rates from the control and perturbed WRF simulations. Results show that the widespread reduction of annual meltwater volume over western North America (Fig. 2a; brown pixels) is associated with small regional increases in low snowmelt rates (Fig. 2b; green pixels), and, critically, a large reduction in high snowmelt rates (Fig. 2d; brown pixels). This is an important new finding, suggesting a tendency for slower snowmelt in a warmer world.

The spatial patterns are nevertheless complex. Decreases in snowmelt rates in all melt rate categories are simulated in the northern Sierra Nevada (California) and the US Pacific Northwest (Oregon and Washington) (Fig. 2b–d). Previous studies have shown that snowpack in these regions is 'at risk'[28,29] due to moderate mid-winter air temperatures that make these regions particularly susceptible to a warming-induced shift from snowfall to rain. At the other end of the spectrum, snowpack at higher elevations and/or colder regions such as the US Intermountain West, Interior Mountains of British Columbia, and the Rocky Mountains is comparatively less sensitive to warming[30] (Fig. 2a). Few regional exceptions to the pattern of reduced high rates of melt include the highest elevations of the Rocky Mountains and Canadian Pacific Ranges, where localized increases in the volume of water produced at high melt rates (Fig. 2d; green pixels) may be explained by warming-induced increases in snowfall[23]. The contrasting results highlight the regional variability and complex nature of snowmelt response to warmer conditions. On average over the regions shown in Fig. 2a (that is, excluding regions of historical SWE <150 mm), total meltwater is projected to decline by 199 mm yr^{-1} or 38%, of which only 15 mm yr^{-1}, or a 5% decline, is explained by a decrease in the volume that occurs at low melt rates (Fig. 2b). The large projected reduction in total meltwater is explained by an average 184 mm yr^{-1} or 33% reduction in the combined volume of meltwater that historically occurred at moderate (Fig. 2c) to high (Fig. 2d) melt rates.

Figure 3 illustrates the percentage of meltwater volume produced at different melt rates. Results show that the majority of meltwater production in regions of historically shallow snowpack occurs at low melt rates (Fig. 3; bottom panel), and, conversely, only a small amount of meltwater production in regions of historically deep snowpack occurs at low rates (Fig. 3; top panel). In all four snow classes (colours in Fig. 3; consistent with grid cells plotted in the map inset of Fig. 1b), warming causes large reductions in the meltwater volume produced at higher snowmelt rates (right set of bars), with corresponding increases in the percentage of meltwater volume produced at lower rates (left set of bars). These results contradict the perhaps intuitive notion that snowmelt rates in a warmer climate will exceed historical values.

Causes of projected changes

To better understand the cause of the projected changes in snowmelt rates, we evaluate the seasonal evolution of simulated and projected snowmelt and snow-cover percentage. Figure 4 shows that the reduction in high melt rates occurs during spring and early summer (top set of coloured lines in Fig. 4), and the increases in low melt rates occur in mid-winter (bottom set of coloured lines in Fig. 4). The reduction in high snowmelt rates is associated with a contraction

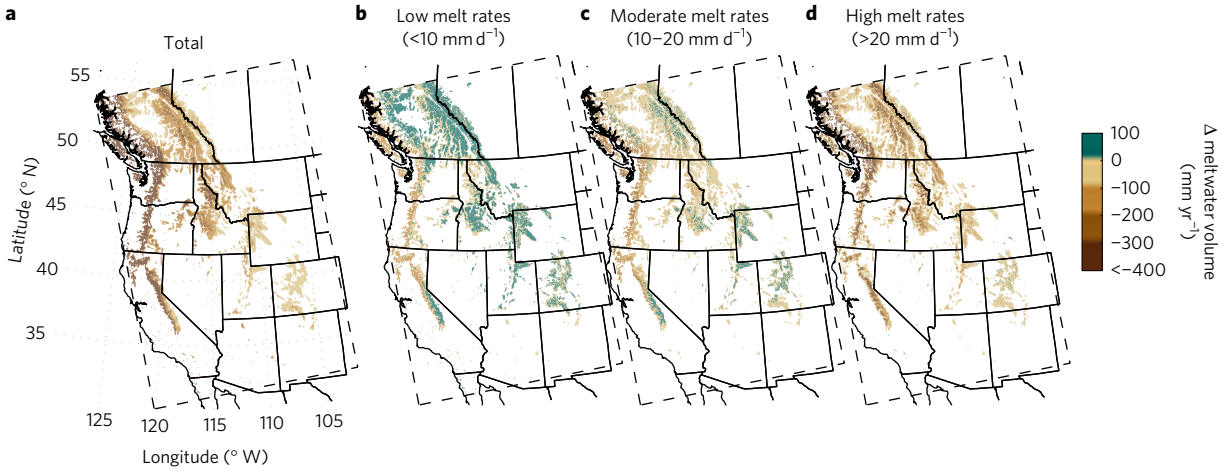

Figure 2 | Reductions in total meltwater volume are primarily associated with reductions in high melt rates. a–c, Maps of the mean annual projected changes in total meltwater volume (mm) (**a**) and the changes that occur at low (<10 mm d^{-1}) (**b**), moderate (10–20 mm d^{-1}) (**c**) and high (>20 mm d^{-1}) (**d**) snowmelt rates. Excluded from the analysis are regions with the historical (2000–2010) mean annual maximum SWE <150 mm (see the inset in Fig. 1b).

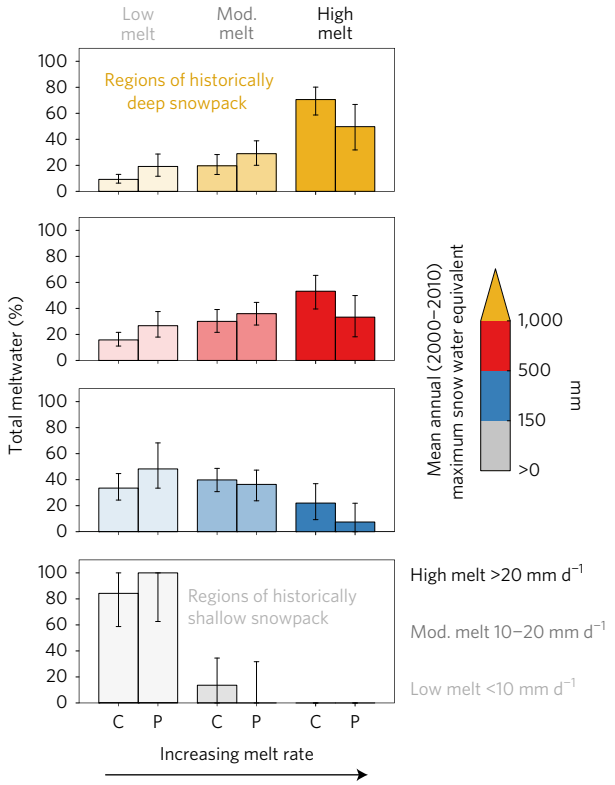

Figure 3 | Changes in the percentage of meltwater volume produced at different melt rates. The median percentage contribution of total snowmelt that occurs at low (<10 mm d^{-1}), moderate (10–20 mm d^{-1}) and high (>20 mm d^{-1}) melt rates (shading; see bins in Fig. 2) by regions binned according to historical snowpack volume (colours as in Fig. 1; see legend), for the control (C) and pseudo-global-warming (P) simulations. The whiskers indicate the interquartile range values.

of the snow season (top set of plots), where reductions in daily snow-cover percentage are skewed toward spring and summer. By contrast, the increase in low melt rates is most pronounced in mid-winter. More generally, there is a tendency towards earlier melt for all melt rate categories and depth classes, as is evident from changes in the centre of mass and the reduced dominance of spring and summertime melt.

Put simply, much more of the land area in the warmer climate scenario is snow-free at times of high energy availability. Figure 5 shows plots of daily sub-canopy surface net radiation (K^*), net turbulent energy (Q^*) and total net energy ($E^* = K^* + Q^*$) simulated for snow-covered grid elements (median values reported) for the control and warmer scenarios. The simulated snow-cover energy balance during spring melt is dominated by net radiation, consistent with previous snowpack energy balance studies (for example, ref. 31). We used a daily E^* threshold of 10 MJ m^{-2} d^{-1} to distinguish the snowpack surface energy required to generate moderate to high snowmelt rates from low melt rates. The mean date on which 10 MJ m^{-2} d^{-1} was first exceeded (Fig. 5; vertical lines in panels) ranged from the first week of April for areas of low snowpack to late-May for areas of deep snowpack. Critically, the historical snow-cover percentage on the date of this energy exceedance is reduced in the warmer scenario by 45% to as much as 64% (Fig. 5; top panels). The results indicate that in a warmer world much less snow-cover will be exposed to high energy fluxes sufficient to drive moderate to high snowmelt rates.

Summary and discussion

We use a mix of historical data analysis and controlled regional climate model simulations to test the hypothesis of slower snowmelt in a warmer world. We have four main conclusions. First, analyses of daily snowpack depletion over western North America demonstrate lower ablation rates in locations with less SWE. The positive relationship between ablation rates and SWE occurs because deeper snowpack persists to late spring and summer when energy availability is high. Second, the widespread simulated reduction of annual meltwater volume over western North America is associated with small regional increases in low snowmelt rates, and, critically, a large reduction in high snowmelt rates. This is an important new finding that contradicts the perhaps intuitive notion that snowmelt rates in a warmer climate will exceed historical values, suggesting a tendency for slower snowmelt in a warmer world. Third, the reduction in high melt rates occurs during spring and early summer, and the increase in low melt rates occurs in mid-winter. The reduction in high snowmelt rates is associated with a contraction of the snow season, where reductions in daily snow-cover percentage are skewed toward spring and summer. Fourth, in a warmer climate, the contraction of spring snow-cover reduces by as much as 64% the snow-covered area that is exposed to net energy sufficient to drive moderate to high snowmelt rates, resulting in slower snowmelt in a warmer world.

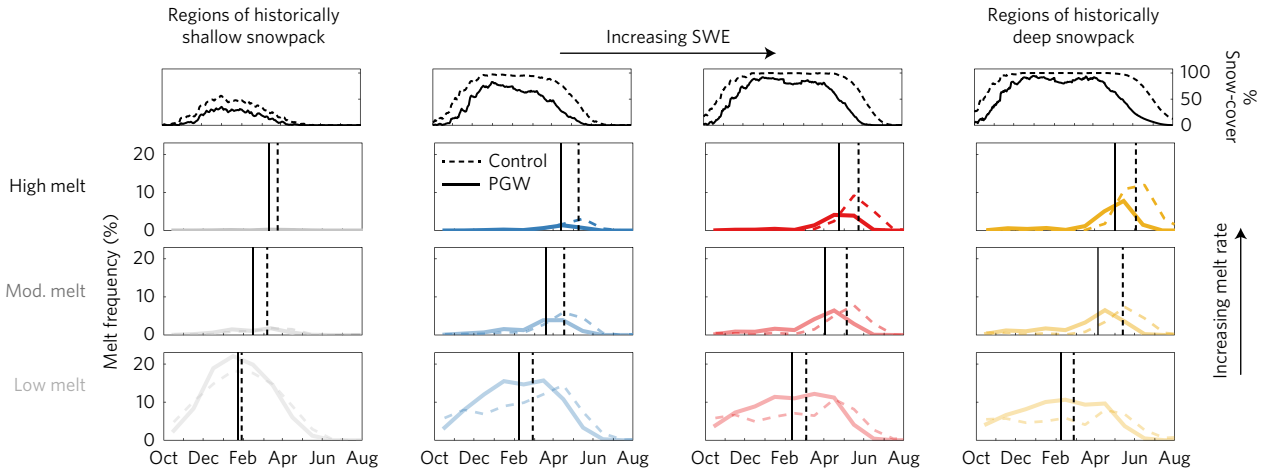

Figure 4 | Large reductions in high melt rates are projected to occur predominantly in regions characterized as having historically deeper snowpack where melt persisted late into the spring and early summer and slight general increases in lower melt rates in winter and early spring. The upper line graphs show the ten-year mean daily snow-cover percentage in grid cells having historical seasonal snowpack characterized as shallow (top-left panel) to deep (top-right panel) for the control (dashed lines) and pseudo-global-warming (solid lines) scenarios. The coloured-line graphs show the 10-year median melt frequency computed as the percentage of total annual snowmelt that occurs in each month at low, moderate and high melt rates (frequencies plotted in each panel column sum to 100%) for the control (dashed lines) and warmer (solid lines) scenarios. The centre of mass is plotted as vertical lines.

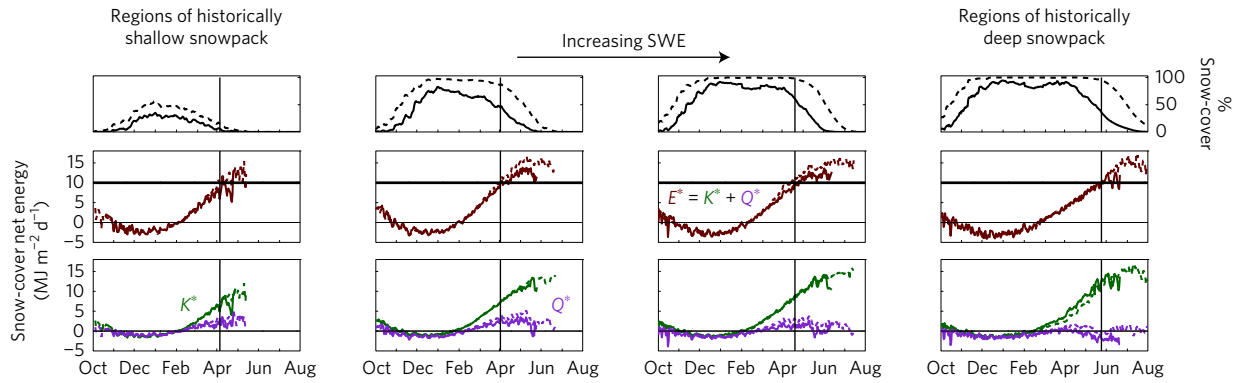

Figure 5 | In a warmer world, less than half of the historical snow-covered area is exposed to net energy >10 MJ m^{-2} d^{-1}—a threshold that approximately divides moderate and high melt rates from lower rates typical of winter and early spring. The column panels and upper line graphs are as in Fig. 4. The daily median net sub-canopy surface energy (MJ m^{-2} d^{-1}) of snow-covered grid cells (E^*; dark red lines; middle row of panels) for the control (dashed lines) and pseudo-global-warming (PGW; solid lines) scenarios are computed as the daily net radiation (K^*; green lines) plus daily net turbulent (Q^*; purple lines) energy (lower row of panels). An E^* threshold of 10 MJ m^{-2} d^{-1} is indicated with the horizontal line across the middle row panels; the vertical lines in all panels indicate the date on which this threshold is first exceeded. The average date of first exceedance of the two scenarios is plotted for clarity.

Large reductions of high spring snowmelt rates in response to climate warming will impact the hydrology of snow-dominated regions, where snowmelt rates are critically linked to streamflow. In particular, slower snowmelt in response to warming may have implications on reduced streamflow and basin water yield. Compared with rainfall, the low-intensity long-duration nature of snowmelt more readily infiltrates soils[32], forming hydrologic connections between hillslopes and water tables[33] that sustain streamflow[34]. High snowmelt rates have been shown to be particularly effective at generating streamflow[17]. Slower snowmelt in a warmer world may decrease the likelihood that wetness thresholds that permit hydrologic connectivity will be exceeded, leading to spring and summer streamflow declines and lower runoff efficiency. For example, slower snowmelt in regions with less SWE may help to explain recent findings[35] that US basins with a lower fraction of precipitation as snow have lower mean annual streamflow. Thus, slower snowmelt has implications on ecological processes sensitive to a timing shift to earlier and reduced snowmelt and streamflow including atmospheric carbon uptake by forests[12], fish survival rates[36,37] and the risk of wildfire[15].

Slower snowmelt in a warmer world will also impact water supply and hydropower production. One hypothesis is that less spring meltwater from reduced snowpack will move less efficiently to downstream reservoirs at a time of increasing seasonal aridity, evaporative demand and socioeconomic needs. Slower snowmelt in a warmer world has unresolved implications on the future risk of spring snowmelt floods. Previous studies have predicted future declines in spring snowmelt floods in the western US[4] and British Columbia, Canada[38], due to simulated reductions in spring snowpack in response to climate warming. While extreme events are not evaluated in the current study, slower snowmelt may be an important mechanism to explain those projected declines in spring snowmelt floods. Conversely, mid-winter increases in melt rates combined with a greater proportion of precipitation falling as rain could locally increase winter flood risk.

Hydrologic implications of slower snowmelt in a warmer world are likely to vary substantially with regional climate, elevation, soil properties, vegetation, evapotranspirative demand, and climate response to changes in greenhouse gas concentrations. Our study is limited to presenting the processes that explain projected changes in snowmelt rates. We report large general declines in spring snowmelt rates over great spatial extents and averaged over a decade—the impact of warming on individual (for example, extreme) melt events may differ. Additionally, warming effects on snowmelt are likely to have more pronounced spatial variability than can be simulated at 4 km grid spacing. For example, topographic shading occurs at much finer scales than simulated here. Earlier snowmelt coincident with a time of lower seasonal sun angles[39] may be slower than we report as a result of terrain shade effects[40]. Given the critical need to better understand the impact of climate change on water resources, future studies are needed to address the myriad hydrological and ecological consequences of less snowfall, reduced seasonal snowpack and a shift toward slower snowmelt.

We identify a mechanism of change in snowmelt rates that impacts snow water resources over much of western North America. While slower snowmelt in a warmer world may appear paradoxical or contrary to the well-accepted idea of water cycle intensification[41], the change is analogous to a downward shift in elevation to a warmer environment where melt rates are historically lower. Such dynamics are evident in historical snowpack observations, where shallower snowpack generally melts earlier and at lower rates than deeper, later-lying snow-cover. The shift to slower snowmelt is caused by warming-induced snow-cover depletion that limits the potential for high snowmelt rates typical of the historical spring and early summer when the snowpack is less likely to freeze overnight, solar insolation is high and snow albedo values are low. The identification of such hydrologic shifts within elevation-driven regional climate regimes is critical as slight perturbations may cause thresholds to be crossed and system behaviour to be indefinitely altered[21]. The implications on streamflow and ecology of large-scale changes in the magnitude of this critical water flux must be better understood to increase climate resilience.

Methods

Methods, including statements of data availability and any associated accession codes and references, are available in the online version of this paper.

Received 2 August 2016; accepted 19 January 2017; published online 27 February 2017

References

1. IPCC *Climate Change 2007: The Physical Science Basis* (eds Solomon, S. *et al*.) (Cambridge Univ. Press, 2007).
2. Beniston, M. Impacts of climatic change on water and associated economic activities in the Swiss Alps. *J. Hydrol.* **412,** 291–296 (2012).
3. Allan, J. D. & Castillo, M. M. *Stream Ecology: Structure and Function of Running Waters* (Springer Science Business Media, 2007).
4. Hamlet, A. F. & Lettenmaier, D. P. Effects of 20th century warming and climate variability on flood risk in the western US. *Wat. Resour. Res.* **43,** W06427 (2007).
5. Mote, P. W., Hamlet, A. F., Clark, M. P. & Lettenmaier, D. Declining mountain snowpack in western North America. *Bull. Am. Meteorol. Soc.* **86,** 39–49 (2005).
6. Barnett, T. P., Adam, J. C. & Lettenmaier, D. P. Potential impacts of a warming climate on water availability in snow-dominated regions. *Nature* **438,** 303–309 (2005).
7. Stewart, I. T., Cayan, D. R. & Dettinger, M. D. Changes in snowmelt runoff timing in western North America under a business as usual climate change scenario. *Climatic Change* **62,** 217–232 (2004).
8. Arnell, N. W. The effect of climate change on hydrological regimes in Europe: a continental perspective. *Glob. Environ. Change* **9,** 5–23 (1999).
9. Harpold, A. A. *et al*. Soil moisture response to snowmelt timing in mixed-conifer subalpine forests. *Hydrol. Process.* **29,** 2782–2798 (2015).
10. Bales, R. C. *et al*. Soil moisture response to snowmelt and rainfall in a Sierra Nevada mixed-conifer forest. *Vadose Zone J.* **10,** 786–799 (2011).
11. Trujillo, E., Molotch, N. P., Goulden, M. L., Kelly, A. E. & Bales, R. C. Elevation-dependent influence of snow accumulation on forest greening. *Nat. Geosci.* **5,** 705–709 (2012).
12. Winchell, T. S., Barnard, D. M., Monson, R. K., Burns, S. P. & Molotch, N. P. Earlier snowmelt reduces atmospheric carbon uptake in midlatitude subalpine forests. *Geophys. Res. Lett.* **43,** 8160–8168 (2016).
13. Rauscher, S. A., Pal, J. S., Diffenbaugh, N. S. & Benedetti, M. M. Future changes in snowmelt-driven runoff timing over the western US. *Geophys. Res. Lett.* **35,** L16703 (2008).
14. Luce, C. H. & Holden, Z. A. Declining annual streamflow distributions in the Pacific Northwest United States, 1948–2006. *Geophys. Res. Lett.* **36,** L16401 (2009).
15. Westerling, A. L., Hidalgo, H. G., Cayan, D. R. & Swetnam, T. W. Warming and earlier spring increase western US forest wildfire activity. *Science* **313,** 940–943 (2006).
16. Westerling, A. L. Increasing western US forest wildfire activity: sensitivity to changes in the timing of spring. *Phil. Trans. R. Soc. B* **371,** 20150178 (2016).
17. Barnhart, T. B. *et al*. Snowmelt rate dictates streamflow. *Geophys. Res. Lett.* **43,** 8006–8016 (2016).
18. Oki, T. & Kanae, S. Global hydrological cycles and world water resources. *Science* **313,** 1068–1072 (2006).
19. McCabe, G. J., Hay, L. E. & Clark, M. P. Rain-on-snow events in the western United States. *Bull. Am. Meteorol. Soc.* **88,** 319–328 (2007).
20. López-Moreno, J., Pomeroy, J., Revuelto, J. & Vicente-Serrano, S. Response of snow processes to climate change: spatial variability in a small basin in the Spanish Pyrenees. *Hydrol. Process.* **27,** 2637–2650 (2013).
21. Trujillo, E. & Molotch, N. P. Snowpack regimes of the Western United States. *Wat. Resour. Res.* **50,** 5611–5623 (2014).
22. Trenberth, K. E. Changes in precipitation with climate change. *Clim. Res.* **47,** 123–138 (2011).
23. Rasmussen, R. *et al*. High-resolution coupled climate runoff simulations of seasonal snowfall over Colorado: a process study of current and warmer climate. *J. Clim.* **24,** 3015–3048 (2011).
24. Liu, C. *et al*. Continental-scale convection-permitting modeling of the current and future climate of North America. *Clim. Dynam.* http://doi.org/bzj8 (2016).
25. Rasmussen, R. *et al*. Climate change impacts on the water balance of the Colorado headwaters: high-resolution regional climate model simulations. *J. Hydrometeorol.* **15,** 1091–1116 (2014).
26. Riahi, K. *et al*. RCP 8.5—A scenario of comparatively high greenhouse gas emissions. *Climatic Change* **109,** 33–57 (2011).
27. Colbeck, S. C. An analysis of water flow in dry snow. *Wat. Resour. Res.* **12,** 523–527 (1976).
28. Nolin, A. W. & Daly, C. Mapping "at risk" snow in the Pacific Northwest. *J. Hydrometeorol.* **7,** 1164–1171 (2006).
29. Dettinger, M. D., Cayan, D. R., Meyer, M. K. & Jeton, A. E. Simulated hydrologic responses to climate variations and change in the Merced, Carson, and American River basins, Sierra Nevada, California, 1900–2099. *Climatic Change* **62,** 283–317 (2004).
30. Mote, P. W. Climate-driven variability and trends in mountain snowpack in Western North America. *J. Clim.* **19,** 6209–6220 (2006).
31. Marks, D. & Dozier, J. Climate and energy exchange at the snow surface in the alpine region of the Sierra Nevada: 2. Snow cover energy balance. *Wat. Resour. Res.* **28,** 3043–3054 (1992).
32. Stephenson, G. R. & Freeze, R. A. Mathematical simulation of subsurface flow contributions to snowmelt runoff, Reynolds Creek Watershed, Idaho. *Wat. Resour. Res.* **10,** 284–294 (1974).
33. Jencso, K. G. *et al*. Hydrologic connectivity between landscapes and streams: transferring reach- and plot-scale understanding to the catchment scale. *Wat. Resour. Res.* **45,** W04428 (2009).
34. Miller, M. P., Buto, S. G., Susong, D. D. & Rumsey, C. A. The importance of base flow in sustaining surface water flow in the Upper Colorado River Basin. *Wat. Resour. Res.* **52,** 3547–3562 (2016).
35. Berghuijs, W., Woods, R. & Hrachowitz, M. A precipitation shift from snow towards rain leads to a decrease in streamflow. *Nat. Clim. Change* **4,** 583–586 (2014).
36. Isaak, D. J. *et al*. Effects of climate change and wildfire on stream temperatures and salmonid thermal habitat in a mountain river network. *Ecol. Appl.* **20,** 1350–1371 (2010).
37. Wenger, S. J. *et al*. Flow regime, temperature, and biotic interactions drive differential declines of trout species under climate change. *Proc. Natl Acad. Sci. USA* **108,** 14175–14180 (2011).
38. Loukas, A., Vasiliades, L. & Dalezios, N. R. Potential climate change impacts on flood producing mechanisms in southern British Columbia, Canada using the CGCMA1 simulation results. *J. Hydrol.* **259,** 163–188 (2002).

39. Musselman, K. N., Molotch, N. P., Margulis, S. A., Kirchner, P. & Bales, R. C. Influence of canopy structure and direct beam solar irradiance on snowmelt rates in a mixed conifer forest. *Agric. Forest Meteorol.* **161C,** 46–56 (2012).
40. Lundquist, J. D. & Flint, A. L. Onset of snowmelt and streamflow in 2004 in the western United States: how shading may affect spring streamflow timing in a warmer world. *J. Hydrometeorol.* **7,** 1199–1217 (2006).
41. Huntington, T. G. Evidence for intensification of the global water cycle: review and synthesis. *J. Hydrol.* **319,** 83–95 (2006).

Acknowledgements

The National Center for Atmospheric Research (NCAR) is sponsored by the National Science Foundation. K.N.M. was supported under an NCAR Advanced Study Program (ASP) Postdoctoral Fellowship. We acknowledge high-performance computing support from Yellowstone (ark:/85065/d7wd3xhc) provided by NCAR's Computational and Information Systems Laboratory, sponsored by the National Science Foundation. We thank N. Addor for thoughtful discussion and M. Barlage for his critical effort to improve the snow simulations.

Author contributions

K.N.M. and M.P.C. designed the study; K.N.M. conducted all analyses; C.L. ran the WRF simulations; K.I. managed the WRF output; K.N.M., M.P.C. and R.R. contributed to the interpretations of the results; and K.N.M. and M.P.C. wrote the paper.

Additional information

Reprints and permissions information is available online at www.nature.com/reprints. Correspondence and requests for materials should be addressed to K.N.M.

Competing financial interests

The authors declare no competing financial interests.

Methods

Station observations. Daily SWE observations for the 1 October 2000–30 September 2010 period at 979 stations in the US and Canada were obtained from the Natural Resources Conservation Service, the California Department of Water Resources, Alberta Environment, and the British Columbia Ministry of Environment. Stations were stratified by the 10-year mean annual maximum SWE: $0 \leq \mathrm{SWE} < 150$ mm (390 station-years), $150 \leq \mathrm{SWE} < 500$ mm (4,330 station-years), $500 \leq \mathrm{SWE} < 1{,}000$ mm (3,070 station-years) and $\mathrm{SWE} \geq 1{,}000$ mm (890 station-years). Ablation rates shown in Fig. 1 were computed as the daily loss of SWE restricted to changes ≤ -1 mm d^{-1} and presented as positive values (losses). The -1 mm d^{-1} value is an estimate of the minimum measurement uncertainty; stations in Canada report SWE to the nearest 1 mm while those in the US report to the nearest 0.1 inch or 2.54 mm. Snowmelt is a difficult flux to measure directly, but is reasonably inferred from the daily depletion of measured snow water equivalent (SWE). We refer to observed SWE depletion as ablation because it implicitly includes both melt and atmospheric moisture exchange (that is, snow surface sublimation and accretion).

WRF control simulations. We analyse a ten-year (October 2000–September 2010) subset of results from a high-resolution (4-km), 13-year retrospective simulation with the Weather Research and Forecasting (WRF) climate model Version 3.4.1 run over much of North America. For detailed model configuration and validation, the reader is referred to ref. 24. Initial and boundary conditions were specified from ERA-Interim reanalysis data[42]. The improved Noah-MP land-surface model[43] simulated the surface energy and water balance including snowpack dynamics and vegetation–snow interactions. Additional improvements to the snow model aimed to reduce a known SWE underestimation included a vegetation-dependent snow-cover depletion curve, allowance for patchy snow in the surface energy balance scheme, and a microphysics-based rain–snow partitioning scheme to replace the more common and subjective temperature-based approach known to introduce much uncertainty in snow models. The Noah-MP physics developments significantly improve the WRF model skill by increasing the seasonal snowpack amount and decreasing cold biases over snow-covered areas[24].

Hourly model output was cropped from the native domain of $1{,}360 \times 1{,}016$ points to a sub-domain of 435×664 grid points (1,740 km east–west by 2,656 km north–south) covering the western US and southwestern Canada and aggregated to daily values (midnight Pacific Standard Time or UTC-8). Model grid cells were stratified according to the simulated 2000–2010 mean annual maximum SWE using the same four bins described previously for the station observations. Note that the land-surface model had an upper SWE limit of 2,000 mm, which was typically exceeded over glaciated regions; because the model did not include glacier dynamics, pixels that met this threshold in any year of either scenario were excluded from analysis.

WRF simulations of a warmer climate. A climate perturbation experiment was conducted to simulate future (2071–2100) climate sensitivity to the Representative Concentration Pathway 8.5 emission scenario[26], in which greenhouse gas emissions continue to increase through the twenty-first century. Similar to the pseudo-global-warming method used in previous WRF runs over Colorado[23,25], warming is simulated by adding the 95-year CMIP5 19-model ensemble-mean temperature, moisture and circulation change signal to the 6-hourly ERA-Interim reanalysis (reanalysis plus a climate perturbation). Details of the model configuration are provided in ref. 24. Model grid cells from the warmer climate simulations were binned according to the historical mean annual maximum SWE as previously described.

WRF snowmelt flux and surface energy terms. We define the daily snowmelt flux as the simulated daily loss of SWE less the daily simulated atmospheric exchange (sublimation and condensation, which are generally $\ll 1$ mm d^{-1}). Hourly fluxes were computed and reported as daily values. As computed, the daily melt flux represents a first-order estimate of the phase-change-derived liquid water that exits the snowpack base in a given time step. By design, the calculation excludes daily rainfall that may percolate through and exit the snowpack in a 24-hour period, but does include rainfall-induced melt. Daily snowmelt fluxes were restricted to non-zero values for analysis. Daily snowmelt classifications were selected roughly following descriptive indices for extreme precipitation[44] where ≥ 10 mm d^{-1} classified as heavy rainfall was used to separate 'low snowmelt' from 'moderate snowmelt' classes and ≥ 20 mm d^{-1} classified as very heavy rainfall was used as the lower bound of the 'high snowmelt' class. The 10 mm d^{-1} division between low and moderate snowmelt rates is very close to the 12.5 mm d^{-1} threshold above which positive streamflow anomalies were reported in ref. 17.

Daily sub-canopy surface net energy E^* was computed as the daily sum of hourly net solar and net longwave radiation emitted from the atmosphere and reflected and emitted from the surface (K^*), and the hourly net turbulent transfer of momentum, heat and water vapour (Q^*). The daily total net energy ($E^* = K^* + Q^*$) term thus excluded the ground heat flux and heat advection by rainfall. All energy terms were computed for snow-covered grid elements (median daily values reported for each snowpack class) for the control and warmer scenarios.

Data availability. The data that support the findings of this study are available on request from the corresponding author. Refer to ref. 24 for information on the availability of the WRF model output.

References

42. Dee, D. *et al*. The ERA-Interim reanalysis: configuration and performance of the data assimilation system. *Q. J. R. Meteorol. Soc.* **137,** 553–597 (2011).
43. Niu, G.-Y. *et al*. The community Noah land surface model with multiparameterization options (Noah-MP): 1. Model description and evaluation with local-scale measurements. *J. Geophys. Res.* **116,** D12109 (2011).
44. Klein Tank, A. M. G., Zwiers, F. W. & Zhang, X. *Guidelines on Analysis of Extremes in a Changing Climate in Support of Informed Decisions for Adaptation* Climate data and monitoring WCDMP-No. 72, WMO-TD No. 1500, 56 (2009).